


Perspective

# On the Experimental Assessment of the Molecular-Scale Interactions between Wood and Water

Nayomi Z. Plaza 

Forest Biopolymers Science and Engineering, USDA Forest Service, Forest Products Laboratory, One Gifford Pinchot Drive, Madison, WI 53726, USA; nayomi.plazarodriguez@usda.gov

Received: 19 June 2019; Accepted: 17 July 2019; Published: 25 July 2019



**Abstract:** Although molecular-scale wood-water interactions needed for moisture-durability can lead to the accelerated development of moisture-durable products, these interactions are often experimentally elusive. In this perspective, the topic's state of the art understanding will be discussed, excluding computational work. Recent research efforts based on infrared spectroscopy methods have provided new insights in terms of the accessibility of the wood polymers and moisture-induced polymer dynamics. Likewise, neutron scattering and nuclear magnetic relaxometry experiments have shown that bound water can be found within more than one local environment inside the cell wall. However, a majority of the experiments have focused on studying extracted or derived polymers instead of unmodified wood. Thus, in this paper some of the questions that still need to be addressed experimentally will also be highlighted.

**Keywords:** molecular scale wood polymer dynamics; conformational changes; bound water; moisture-induced structural changes

## 1. Introduction

The presence of water in wood can lead to structural changes across various length scales [1–8]. Moreover, it can also increase the mobility of wood polymers [9–11], which can facilitate moisture-induced relaxations [12,13] and facilitate ion transport [14]. Despite the important role that molecular-scale wood-water interactions play in bulk-scale processes like softening and diffusion of ions, which ultimately affect the wood's durability and performance, our fundamental understanding of these molecular interactions is rather incomplete.

Research efforts aiming to improve our understanding of sorption phenomena in this regime are often limited by the available technology. Only a few techniques can access the length and time scales pertaining to molecular interactions (Figure 1), namely nuclear magnetic resonance (NMR), infrared spectroscopy (IR) methods, neutron scattering and diffraction (via neutrons or x-rays), and dielectric relaxation spectroscopy (DRS). In addition, when measuring wood, researchers using these techniques must overcome poor contrast between the wood polymers signal and non-trivial data analysis due to overlapping of signals from the wood polymers. Nevertheless, research endeavors focused on better understanding changes in hydrogen bonding upon hydration and accessibility to water have been increasing in the past few years [15–20]. Nuclear magnetic resonance (NMR) and Fourier-transform infrared spectroscopy (FTIR) have been increasingly used to study the effects of moisture-uptake in the chemical structure and accessibility of the wood polymers, with most studies focusing on cellulose [15,16,21]. X-ray diffraction (XRD) methods have provided insights on the moisture-induced changes in cellulose at the crystalline lattice level [8]. Changes in the polymer dynamics due to water absorption have also been studied, yet most efforts have only quantified the increased polymer mobility

in terms of  $T_1$  relaxation times [15,16] and trends in the secondary relaxations [22]. Quasielastic neutron scattering (QENS) have further quantified the polymer mobility in terms of the mean square displacement (MSD) [10,23]. The water dynamics associated to the increased polymer mobility have been easier to probe. NMR, FTIR, and QENS experiments have provided evidence that water in wood can be found in more than one local environment, i.e., interactions with hydrophilic polymers or with other water molecules [20,24–26]. Yet, only a few experiments have quantified the water dynamics of bound water in wood [26].

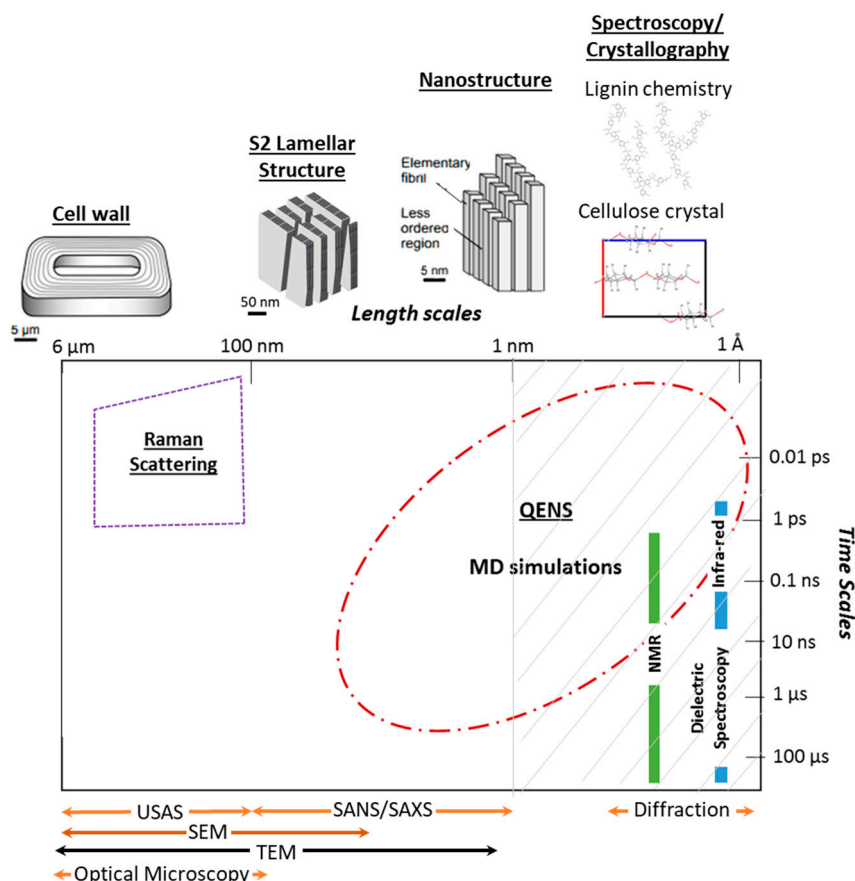


**Figure 1.** Conventional techniques used to study wood across several length and time scales. The relevant wood structure is included for comparison purposes. This perspective focuses on the molecular-scale interactions. The techniques applicable can probe length scales from 1 nm to 1 Å and time scales from 0.01 ps to 100 μs. Techniques listed in the figure (from left to right) include: ultra-small angle scattering (USAS), small angle neutron scattering (SANS) and small angle x-ray scattering (SAXS), scanning electron microscopy (SEM), transmission electron microscopy (TEM), quasielastic neutron scattering (QENS), molecular dynamics (MD) simulations, and nuclear magnetic resonance (NMR). Figure adapted from Martinez-Sanz et al. [27].

In this perspective, I will provide a brief review of the current research trends on this topic, excluding recent research efforts based solely on Molecular Dynamics (MD) simulations and other computational methods. First, due to the interdisciplinary nature of the field, I provide a section providing a brief description of the terminology used in this paper. Then, the paper is divided into moisture-induced changes in the structural and temporal regime. Finally, I discuss questions that still need to be addressed by future research.

## 2. Relevant Terminology

The purpose of this section is to provide clarity with regards to the nomenclature used in this paper. Due to the interdisciplinary nature of wood science research, terms such as nanofibrils, elementary fibrils, and microfibrils are often used interchangeably. Thus, a brief description of the term unmodified wood and its components is provided below. Details about the biosynthesis of the polysaccharides and the lignification process are out of the scope of this paper and are therefore not included in this section.

### *Unmodified Wood*

Unmodified wood refers to wood that has not been heat treated or chemically modified in order to alter the properties of the material. The term includes wood that has been kiln dried and/or vacuum dried, and is often referred to in the literature as native wood. Native wood can be divided into softwoods and hardwoods depending on the species. At the growth ring level, it can be further divided into earlywood and latewood [28]. Moreover, it can also be classified as normal, compression, or tension wood depending on the material source (i.e., branches versus trunk). These classifications are important to consider because they will affect the cell wall thickness, density, and cellular structure of the studied sample. Thus, these variations can change among other things the volume probed by scattering and spectroscopy methods and ultimately impact the overall measured intensity. The main components of unmodified wood are listed and briefly described below.

1. Cellulose accounts for 40%–45% of the cell wall in softwoods and 38%–49% in hardwoods [29]. In unmodified wood, cellulose is found in the cellulose microfibrils, which are bundles of cellulose elementary fibrils that are formed by an ordered arrangement of 18 to 24 chains. Only non-crystalline cellulose is accessible to water and at the elementary fibril level only surface chains are thought to be accessible [30]. Cellulose is a linear polysaccharide whose primary unit is the cellobiose. Each primary unit consists of two glucose units linked by a  $\beta(1 \rightarrow 4)$  glycosidic bond [29]. Cellulose in higher order plants can be naturally found in two crystalline forms, namely  $I_\alpha$  and  $I_\beta$  [31]. The main differences between the two allomorphs are hydrogen bonding, crystal stacking and number of cellulose chains per crystal. In the triclinic cellulose  $I_\alpha$  there is only one cellulose chain per crystal and the crystals are stacked longitudinally by glucose units that vary slightly in conformation. This allomorph is generally found as the dominant crystalline phase in bacterial cellulose and algae [32,33]. In the monoclinic cellulose  $I_\beta$  there are two alternating cellulose chains held together by intramolecular hydrogen bonds in each crystal and its crystals are stacked paralleled to each other by forming inter-molecular hydrogen bonds. While spectroscopy studies have suggested that both forms of cellulose  $I$  can coexist in the native plants [32,34], the dominant crystalline form in wood is  $I_\beta$  [33,35]. The monoclinic  $I_\beta$  structure found in wood is typically described in terms of the  $a$ ,  $b$ ,  $c$ , and  $\gamma$  lattice parameters, which can be solved by tracking the main diffraction peaks, namely the (200), the (110), the (110), and (004) [8,32,36]. The longitudinal axis of the cellulose fibers is parallel to the  $c$ -axis. The cellulose chains are hydrogen-bonded into planar sheets along the  $b$ -axis, and these sheets are stacked via Van der Waal interactions along the  $a$ -axis. Most evidence supports that cellulose has both hydrophilic and hydrophobic surfaces [6], with the (110), (010), and (110) planes being the most hydrophilic ones [37]. Although the degree of cellulose crystallinity can vary across wood species and measuring methods, values between 50 to 65% are typical for both softwoods and hardwoods [38]. The remaining cellulose is typically considered amorphous or para-crystalline, which is an intermediate phase between  $I_\alpha$  and  $I_\beta$ , and is more laterally disordered and mobile than crystalline cellulose [6,39].
2. Hemicelluloses can be found in the middle lamella that holds together wood cell walls as well as inside the matrix of the cell walls [40]. It usually accounts for 15%–25% of the wood's dry weight [29]. Hemicelluloses are polysaccharides with a lower degree of polymerization than cellulose. Usually, they have an equatorial  $\beta$ -1,4-linked glycosyl residue backbone [41] and despite

its backbone structure similarities to cellulose it lacks crystallinity. The specific composition of the hemicelluloses can vary across wood types, species, and even wood cell walls [42]. The main hemicellulose in hardwoods is xylan and in softwoods it is galactoglucomannan [43]. In softwoods, xylan is typically found in the primary wall [41], while the major hemicellulosic components found in the secondary cell are partially acetylated galactoglucomannans and arabinoglucuronoxylan [44]. Different hemicelluloses have varying degrees of affinity between cellulose and lignin and hence they act as a bridge between the two components [45]. For instance, glucomannans have a higher affinity to cellulose than xyans [46], whereas xyans associate mostly with lignin [46] despite their ability to interact with cellulose hydrophobic surfaces [47]. Hemicelluloses are much more accessible to water than cellulose. In the hemicelluloses, it is assumed that most of all of its hydroxyl groups are accessible because of its lack of crystallinity [48] and the estimated concentration of available hydroxyl groups ranges from 8.6 to 18.8 mmol/g in glucomannan, whereas in xylan is 14.4 mmol/g [30].

3. Lignin is a three-dimensional aromatic polymer network that usually accounts for 26%–34% of the wood dry weight in softwoods and 23%–30% in hardwoods [29]. It is made of phenylpropane units that are linked by ether and carbon-carbon bonds [29,49]. In the cell wall lignin is typically formed after polysaccharide synthesis and thus its supramolecular structure is determined by the space available when lignin is deposited, meaning that middle lamella lignin differs from secondary cell wall lignin [50]. In the middle lamella, lignin is thought to form 3D globules made of folded chain oligolignols, whereas in the secondary cell wall it forms tubular structures that surround the hemicellulose coated microfibrils. Recent evidence, based on molecular dynamics simulations, have also suggested that the aromatic rings of lignin align themselves parallel to the cellulose fibrils; though this order seems limited to the first monolayer of lignin [51]. Due to its lack of crystallinity, it is expected that most of its hydroxyl groups will be available to water [48]. Nonetheless, lignin is the least hydrophilic wood polymer and its concentration of accessible hydroxyl groups is comparable to the theoretical accessibility of cellulose [30].
4. Water in wood can exist as bound water and free water. The total amount of water in wood is called the moisture content and it is defined as the mass of water over the mass of oven dried wood [1]. The equilibrium moisture content varies according to the environmental conditions, such as relative humidity (RH) and temperature. In wood science, bound water typically refers to water that is bound within the wood cell wall by intermolecular attractions and free water refers to water that is found within empty cavities inside the wood structure, such as lumina and pits [1]. Different groups have proposed that water within wood can be found in two or three states [52]. While, it has been shown that the freezable bound water found via differential calorimetry measurements is caused by sample preparation [53], some scattering techniques have been able to discern between populations of water molecules that have different types of local environment. Hence, in this paper, all bound water will be referred to as absorbed water. It is known that changes in the local environment experienced by water molecules affect their properties and state [54]. In the literature, water that interacts strongly with the wood polymers has been referred to as slow water, strongly-bonded water, and, in some instances, non-freezing water. Here, it will be referred to as strongly-bound water. Water that interacts loosely with the wood polymers and/or is more likely interacting with other water molecules has been referred to as fast water, weakly-bonded water, and/or bulk-like water. Here, the term loosely-bound water will be used.
5. Extractives correspond to non-structural components that can be typically removed with solvents. These components are typically classified into three subgroups: aliphatic compounds, terpenes, terpenoids, and phenolic compounds [55]. Although, the total content and composition of these components can vary greatly between species and even within different parts of a tree, the majority of the extractives are typically found in the heartwood [44]. In general, extractives account for 2% to 10% of the wood's dry mass, although some durable species can have higher

values [55]. It is widely accepted that extractives play a role in increasing the durability of wood, particularly, in terms of decay and termite resistance [56]. Moreover, studies on the bulk swelling of wood in organic liquids have shown that extractives can lower the rate of maximum swelling [55]. However, in situ studies focusing on the effect of the extractives on the molecular-scale interactions between wood and water have been difficult likely due to the variability in content and composition of the extractives. NMR experiments have shown that wood with higher content of wood extractives have different bound water  $T_2$  values than other temperate species [57], yet it is still unclear whether the extractives play a role in the dynamics of the bound water or the mobility of the wood polymers.

### 3. Moisture-Dependent Behavior of the Wood Polymers

Even though moisture uptake in wood leads to structural changes across multiple length scales, this discussion will focus only on those changes that pertain the molecular and nanoscale levels. Research at these length scales have focused on improving our understanding of moisture-induced conformational changes in the wood polymers, mainly in terms of hydrogen bonding and water accessibility, as well as changes in the crystal and chemical structure. The majority of the studies have focused on extracted polysaccharides and model systems made out of cellulose nanofibrils and/or bacterial cellulose; only a few studies have aimed to study wood in its entirety.

Synchrotron XRD studies have provided insights on the changes that occur at the cellulose crystalline lattice level. More specifically, studies on spruce earlywood wood cells have shown that the cellulose crystalline lattice is compressed upon increasing hydration [8]. This change has been attributed to (a) an increase in the swelling pressure exerted by the surrounding matrix [36] and (b) to compressive stresses caused by the condensation and evaporation of ordered layers of water molecules on the hydrophilic surfaces of the elementary fibrils [8]. While the hydration dependence of the XRD profiles has been shown for different wood species by different research groups [6,36,58,59], thorough quantification of the hydration effects on the cellulose crystalline lattice has been limited to earlywood spruce [8]. An increased number of studies have focused instead on the determination of the cellulose crystallinity index via FTIR, NMR, XRD, and even fluorescence microscopy methods [38,60,61], but only a few studies have addressed the moisture-dependence of the crystallinity index [58,59].

Solid state NMR and FTIR studies have provided insights on the moisture sorption phenomena, particularly in terms of which hydroxyl sites are accessible to vapor exchange. A combination of  $^2\text{H}$  Magic-angle spinning (MAS) NMR and FTIR spectra have been used to show that only two of the three theoretically available hydroxyl groups on the surface of cellulose fibrils from microcrystalline cellulose derived from cotton linters are accessible to surrounding water molecules [15]. By combining these experiments with MD simulations, the researchers were even able to confirm that the  $^1\text{HO}(3)$ ,  $^1\text{HO}(2)$ , and  $^1\text{HO}(6)$  groups all share about as many hydrogen bonds with water. However, hydrogen exchange at the  $^1\text{HO}(3)$  groups, which act as acceptors of water, have a much slower rate of exchange than the  $^1\text{HO}(2)$  and  $^1\text{HO}(6)$  groups, which act as donors to water. Interestingly, these findings were in agreement with earlier MD simulations [62] that were much shorter (1 ns vs 10 ns). FTIR studies on hemicelluloses films made out of glucomannan from *Amorphophallus Konjac* and rye arabinoxylan showed that even at high RH 15% of the hydroxyl groups were still not accessible to exchange by  $\text{D}_2\text{O}$  vapor [21]. Moreover, while no preferential sites were observed in xylan, the  $\text{O}(6)\text{H}$  group was the most accessible in glucomannan.

Insights on the mechanisms behind the moisture-induced polymer dynamics have been more elusive experimentally. While it is widely accepted that moisture-uptake can lead to increase mobility of the wood polymers, experimental studies on this topic have been mostly limited to NMR spectroscopy, dielectric relaxation spectroscopy (DRS), and more recently quasielastic neutron scattering (QENS) of model systems and extracted polysaccharides.  $^{13}\text{C}$  CP MAS NMR studies on cellulose derived from cotton have shown that the molecular motions of the  $\text{C}-^1\text{HO}(2)$  groups are slower than those of the  $\text{C}-^1\text{HO}(6)$  groups because they are more constrained [15]. Similar experiments performed on



nanocomposites made from cellulose nanofibrils (CNF) and xyloglucan (XG) from tamarind seeds have shown that increased water content and chain mobility in XG shifts the  $^{13}\text{C}$  relaxation spectra to shorter times [16]. As expected, this effect is more pronounced in bulk XG than in bulk CNF. Interestingly, the XG in the composite exhibited much slower polymer mobility than in the neat XG, probably due to having a much more rigid backbone. Moreover, the dynamics of distinct  $^{13}\text{C}$  sites were tracked at two different hydration levels in terms of their  $T_1$  values and relaxation rates; it was found that for CNF the C4sa and C6sa from the surface/amorphous peaks became more mobile when hydrated while the C6c became slower. In XG, all sites had some increased mobility and the most mobile site was C6sa. However, while these studies have provided robust evidence showing which sites become more mobile, they only quantified the observed increased mobility in terms of  $T_1$  values and their relaxation rates. QENS studies on bacterial cellulose [10] and lignin from vanilla beans [23], on the other hand, have been able to quantify the increased mobility due to hydration in terms of the mean squared displacement (MSD) of the polymers, a quantity that can easily be calculated from MD simulations. Likewise, QENS experiments on loblolly pine latewood showed that the overall mobility of the in-situ wood polymers increased with increasing RH, yet no average MSD could be derived from these studies [26].

Dielectric relaxation spectroscopy measurements have also been extensively used to describe the mobility of the wood polymers [22]. Below, the glass transition temperature and three relaxation processes are observed in dry polysaccharides, i.e., the  $\beta$  relaxation due to local main chain motion, the  $\gamma$  relaxation caused by side groups motion, and the  $\delta$  relaxation due to local chain motions in a hydrated polysaccharide phase [63] or as a precursor to a structural relaxation [64]. Hydrated polysaccharides also exhibit a  $\beta_{\text{wet}}$  relaxation, whose origin is still debated. Most evidence, however, suggests that this relaxation corresponds to the motion of a gel-like polymer-water network [63]. DRS studies generally show that the relaxation processes change with the addition of water as both the activation energy and the cooperativity between local chains increase [22]. More recently, the effect of the state of the absorbed water on the secondary dielectric relaxations observed in cellulose was investigated using DRS and Low-Field NMR [20]. This study showed that even though the dielectric strength exhibited a moisture-dependence in all relaxations ( $\beta$ ,  $\beta_{\text{wet}}$  and  $\gamma$ ), only the  $\gamma$  and the  $\beta$  had increased activation energy with increasing hydration (from 0 to 28% MC). Although these studies have provided valuable insights on the temperature and humidity dependence of the secondary relaxations, the dynamics of the polymers have not been quantified.

A summary of the studies focused on moisture-induced behavior of the wood polymers is listed below in Table 1.

**Table 1.** Summary of studies on the moisture-dependent behavior of the wood polymers.

Material Studied	Experimental Techniques Used	Findings
Spruce Earlywood sections	Synchrotron X-ray Diffraction (XRD)	Measured compression of the cellulose crystalline lattice with increasing hydration [8].
Various wood species	Cu K $\alpha$ XRD	Showed moisture-induced changes in the XRD diffraction profiles [6,36,58,59], including increased crystallinity [58,59].
Microcrystalline cellulose from cotton	$^2\text{H}$ Magic-angle spinning nuclear magnetic resonance (MAS NMR) and Fourier-transform Infrared (FTIR) Spectroscopy MD simulations were also used in analysis of the data.	Provided evidence that only two hydroxyl sites on the surface of the cellulose were accessible to water molecules [15].

Material Studied	Experimental Techniques Used	Findings Findings
Hemicelluloses films from rye arabinoxylan and Konjac glucomannan	FTIR	Accessibility of hydroxyl sites to D <sub>2</sub> O vapor exchange [21].
Microcrystalline cellulose from cotton	<sup>13</sup> C Cross-polarization Magic-angle Spinning (CP MAS) NMR	Tracked T <sub>1</sub> values quantify molecular motions [15].
Nanocomposites made from cellulose nanofibrils (CNF) and tamarind xyloglucan (XG)	<sup>13</sup> C CP MAS NMR	Quantified increased molecular mobility of CNF and XG via tracking the T <sub>1</sub> values and relaxation rates [16].
Bacterial cellulose [10] and lignin from vanilla beans [23]	Quasielastic neutron scattering (QENS) combined with MD simulations	Tracked increase in mobility in terms of the mean square displacement of the polymers as a function of hydration level.
Loblolly pine latewood	QENS	Showed that overall mobility increased but no average mean square displacement (MSD) was calculated [26].
Various polysaccharides including cellulose	Dielectric relaxation spectroscopy (DRS), and low-field NMR	DRS showed that increasing the moisture content leads to increased activation energy and cooperativity between local chains [22]. For cellulose, all relaxations ( $\beta$ , $\beta_{wet}$ and $\gamma$ ) exhibited a moisture-dependence [20].

#### 4. State of Water Absorbed in Wood and Wood Polymers

Though several experimental techniques have been used to quantify the wood-moisture relations [65], only a few studies have aimed to improve our understanding on the state of absorbed water in wood. Despite the increasing research efforts in this topic, most studies have focused on cellulose and have provided limited information describing the state of water in terms of its diffusion, molecular association to the wood polymers, and/or nanoscale water distribution in the cell wall.

Previously, two-dimensional T<sub>1</sub>–T<sub>2</sub> 1H NMR measurements showed that absorbed water in spruce had two different spin relaxation times (T<sub>1</sub>). These results were attributed to water being found in two local environments: less mobile water responsible for the swelling of the wood polymers and mobile water possibly found in small voids within the cell wall [52]. More recently, NMR <sup>2</sup>H relaxometry experiments on nanocomposites made out cellulose nanofibrils (CNF) and tamarind xyloglucans (XG) were carried out to learn about the water dynamics in these polymers [16]. These studies have shown that water tends to be less mobile in neat XG than in the CNF, which was attributed to differences in the water distribution. In the neat XG, water is expected to be distributed throughout the polymer, thus limiting the amount of water that interacts with other water molecules, which would be more mobile, whereas in the CNF water is only absorbed at the surface of the fibrils. As expected the water dynamics in the CNF/XG interphase were higher than those observed in the neat CNF. Similarly, low-field NMR studies have suggested that water in cellulose extracted from corn can exist in three different states: tightly-bound, freezable loosely-bound, and non-freezable loosely-bound [20]. By combining the NMR results with DRS, it was found that the freezable loosely-bound water, which was described as water that is not directly bonded to the cellulose, but is found within the first couple hydration layers, did not affect any of the relaxations under study. Furthermore, it was found that tightly-bound water was incorporated into the relaxation unit in all relaxations observed but only affected the dynamic behavior of  $\beta$ . Whereas the non-freezable loosely-bound water acted as a plasticizer in all secondary relaxations ( $\beta$ ,  $\beta_{wet}$  and  $\delta$ ). Micro-FTIR studies on ginkgo biloba have also shown that absorbed

water can exist in three states, namely, strongly bonded, moderately bonded, and weakly bonded to hydrogen [25]. In this study, strongly bonded water included water bound directly by hydrogen bonds to the hydrophilic wood polymers as well as tetrahedral coordinated water molecules that were strongly interacting with other water molecules. Thus, it includes both water that is tightly-bound and loosely-bound (as described via NMR and QENS studies). It was found that below 40% RH most water was described as strongly bonded, whereas from 40 to 60% RH water tended to be weakly bonded. Beyond 60% RH the strongly bonded component increased faster than the weakly-bonded one, which was believed to be caused by an increase in the number of water molecules that interacted with other water molecules to form five-molecule tetrahedral structures. While these studies provided valuable insights on the local environments experienced by water upon interacting with wood and its extracted polymers, the water dynamic properties were not accessible.

Neutron spectroscopy measurements like QENS have been successful in quantifying the elusive water dynamics and have found that absorbed water in loblolly pine latewood [26] and bacterial cellulose (BCC) [24] can be described as jump diffusion [66], which in MD simulations has been called a stop and go process [18]. Two water populations were observed in both lignocellulosic systems, in BCC only the narrow component dynamics were accessible, which were attributed to hydration water that became mobile between 220 K and ~260 K. Conversely, in wood, the water dynamics of both the tightly-bound and loosely-bound water were quantified; it was found that the residence time of both water types decreased with humidity while the diffusion coefficient increased. This trend was most noticeable above 60% RH in the tightly-bound water, whose diffusive motion was an order of magnitude slower than the motion of the loosely-bound water. Furthermore, the relative amount of loosely-bound water increased with increasing humidity, which was attributed to water clusters that increased in size. Moreover, the QENS studies on wood also revealed that the radius of confinement experienced by the absorbed water molecules, which ranged from 3 to 6 Å with increasing RH (3.5% to 98%) was comparable to the smallest size detected via NMR cryoporometry experiments, which accounted for over 70% of the total porosity in wood cell walls [67].

A summary of the studies discussed in this section is listed below in Table 2.

**Table 2.** Summary of studies focused on the state of water absorbed in wood and its polymers.

Material Studied	Experimental Techniques Used	Findings
Spruce	2D T <sub>1</sub> -T <sub>2</sub> <sup>1</sup> H Nuclear Magnetic Resonance (NMR)	Found two different spin relaxation times, attributed to less mobile water capable of swelling wood, and mobile water in voids [52].
Nanocomposites made out of cellulose nanofibrils (CNFs) and tamarind xyloglucan (XG)	NMR <sup>2</sup> H relaxometry	Found that water is less mobile in XG than CNFs and their water distribution is also different [16].
Cellulose extracted from corn	Low-field NMR and dielectric relaxation spectroscopy (DRS)	Found evidence for three populations of water: tightly-bound, which was found incorporated in all relaxation units, freezable loosely-bound, and non-freezable loosely-bound, which acted as a plasticizer [20].
Gingko biloba	Micro Fourier-transform infrared spectroscopy (FTIR)	Found three water populations: strongly bonded, moderately bonded, and weakly bonded to hydrogen. The relative content of the water populations changed with humidity [25].
Bacterial cellulose	Quasielastic neutron scattering (QENS) and Molecular Dynamics (MD) simulations	Found two water populations and described the dynamics of one using a jump diffusion model [24].
Loblolly pine latewood	QENS	Found two water populations: tightly-bound and loosely-bound water. The diffusive behavior of both populations was quantified using a jump diffusion model [26].



## 5. Needs for Future Research

Recent research efforts have focused mainly on studying the effects of moisture uptake on the wood polymers, mostly cellulose. More experimental studies that probe the unmodified wood as a whole are still needed. At the molecular level, extracted polymers may not be as comparable to the in-situ wood polymers and experiments that can confirm similarities or differences between them in terms of their mobility, accessibility, swelling, and/or bound water dynamics are needed. Additionally, experimental studies that focus on determining if there are molecular-scale components to the sorption hysteresis would be valuable. Likewise, chemical modifications meant to improve the durability against moisture and/or decay are likely to affect the molecular-scale wood-water interactions, i.e., experiments that can provide some insights on this topic are needed.

Given the increasing trend in studying molecular-scale phenomena using computational methods, it is evident that more experiments that can probe the same time and length scales accessible to simulations are needed so that experimental data can validate the models proposed related to moisture sorption phenomena. It would be useful if we can measure quantities that can be calculated via simulations (i.e., MSD) and/or we can measure signals that can also be derived from the polymer structure used in simulations (i.e., XRD profiles; NMR or neutron scattering data). Likewise, due to the complexity of the experimental data pertaining the molecular-scale structural and temporal changes, more efforts that include complementary techniques are needed to deconvolute the signal acquired, not just simulations to aid in the analysis but also techniques that can probe similar time and length scales. Lastly, many experiments study the equilibrated conditioned structure probably due to long data acquisition times. Thus, time-resolved studies that can study the transient changes before equilibrium is reached are still needed.

**Funding:** This research received no external funding.

**Conflicts of Interest:** The author declares no conflict of interest.

## References

1. Glass, S.V.; Zelinka, S.L. Moisture relations and physical properties of wood. In *Wood Handbook: Wood as an Engineering Material*; U.S. Dept. of Agriculture, Forest Service, Forest Products Laboratory: Madison, WI, USA, 2010; pp. 4.1–4.19.
2. Stamm, A.J. SHRINKING and SWELLING of WOOD. *Ind. Eng. Chem.* **1935**, *27*, 401–406. [[CrossRef](#)]
3. Rafsanjani, A.; Stiefel, M.; Jefimovs, K.; Mokso, R.; Derome, D.; Carmeliet, J. Hygroscopic Swelling and Shrinkage of Latewood Cell Wall Micropillars Reveal Ultrastructural Anisotropy. *J. R. Soc. Interface* **2014**, *11*, 20140126. [[CrossRef](#)] [[PubMed](#)]
4. Derome, D.; Griffa, M.; Koebel, M.; Carmeliet, J. Hysteretic Swelling of Wood at Cellular Scale Probed by Phase-Contrast X-Ray Tomography. *J. Struct. Biol.* **2011**, *173*, 180–190. [[CrossRef](#)] [[PubMed](#)]
5. Jakob, H.F.; Tschegg, S.E.; Fratzl, P. Hydration Dependence of the Wood-Cell Wall Structure in Picea Abies. A Small-Angle X-Ray Scattering Study. *Macromolecules* **1996**, *29*, 8435–8440. [[CrossRef](#)]
6. Fernandes, A.N.; Thomas, L.H.; Altaner, C.M.; Callow, P.; Forsyth, V.T.; Apperley, D.C.; Kennedy, C.J.; Jarvis, M.C. Nanostructure of Cellulose Microfibrils in Spruce Wood. *Proc. Natl. Acad. Sci* **2011**, *108*, E1195–E1203. [[CrossRef](#)]
7. Plaza, N.Z.; Pingali, S.V.; Qian, S.; Heller, W.T.; Jakes, J.E. Informing the Improvement of Forest Products Durability Using Small Angle Neutron Scattering. *Cellulose* **2016**, *23*, 1593–1607. [[CrossRef](#)]
8. Zabler, S.; Paris, O.; Burgert, I.; Fratzl, P. Moisture Changes in the Plant Cell Wall Force Cellulose Crystallites to Deform. *J. Struct. Biol* **2010**, *171*, 133–141. [[CrossRef](#)]
9. Kuttich, B.; Grefe, A.K.; Kröling, H.; Schabel, S.; Stühn, B. Molecular Mobility in Cellulose and Paper. *RSC Adv.* **2016**, *6*, 32389–32399. [[CrossRef](#)]
10. Petridis, L.; O'Neill, H.M.; Johnsen, M.; Fan, B.; Schulz, R.; Mamontov, E.; Maranas, J.; Langan, P.; Smith, J.C.; Neill, H.M.O.; et al. Hydration Control of the Mechanical and Dynamical Properties of Cellulose. *Biomacromolecules* **2014**, *15*, 4152–4159. [[CrossRef](#)]

11. Bellissent-Funel, M.C. *Hydration Processes in Biology: Theoretical and Experimental Approaches*; NATO Science Series, Series A, Life sciences; v. 305; IOS Press: Amsterdam, The Netherlands, 1999; ISBN 9789051994391.
12. Cousins, W.J. Young's Modulus of Hemicellulose as Related to Moisture Content. *Wood Sci. Technol.* **1978**, *12*, 161–167. [[CrossRef](#)]
13. Lenth, C.A.; Kamke, F.A. Moisture Dependent Softening Behavior of Wood. *Wood Fiber Sci.* **2001**, *33*, 492–507.
14. Zelinka, S.L.; Gleber, S.C.; Vogt, S.; López, G.M.R.; Jakes, J.E. Threshold for Ion Movements in Wood Cell Walls below Fiber Saturation Observed by X-Ray Fluorescence Microscopy (XFM). *Holzforschung* **2015**, *69*, 441–448. [[CrossRef](#)]
15. Lindh, E.L.; Bergenstråhle-Wohlert, M.; Terenzi, C.; Salmén, L.; Furó, I. Non-Exchanging Hydroxyl Groups on the Surface of Cellulose Fibrils: The Role of Interaction with Water. *Carbohydr. Res.* **2016**, *434*, 136–142. [[CrossRef](#)] [[PubMed](#)]
16. Terenzi, C.; Prakobna, K.; Berglund, L.A.; Furó, I. Nanostructural Effects on Polymer and Water Dynamics in Cellulose Biocomposites: <sup>2</sup>H and <sup>13</sup>C NMR Relaxometry. *Biomacromolecules* **2015**, *16*, 1506–1515. [[CrossRef](#)] [[PubMed](#)]
17. Chen, P.; Terenzi, C.; Furó, I.; Berglund, L.A.; Wohlert, J. Hydration-Dependent Dynamical Modes in Xyloglucan from Molecular Dynamics Simulation of <sup>13</sup>C NMR Relaxation Times and Their Distributions. *Biomacromolecules* **2018**, *19*, 2567–2579. [[CrossRef](#)] [[PubMed](#)]
18. Kulasinski, K.; Guyer, R.; Derome, D.; Carmeliet, J. Water Diffusion in Amorphous Hydrophilic Systems: A Stop and Go Process. *Langmuir* **2015**, *31*, 10843–10849. [[CrossRef](#)]
19. Kulasinski, K.; Guyer, R.; Ketten, S.; Derome, D.; Carmeliet, J. Impact of Moisture Adsorption on Structure and Physical Properties of Amorphous Biopolymers. *Macromolecules* **2015**, *48*. [[CrossRef](#)]
20. Zhao, H.; Chen, Z.; Du, X.; Chen, L. Contribution of Different State of Adsorbed Water to the Sub-T<sub>g</sub> Dynamics of Cellulose. *Carbohydr. Polym.* **2019**, *210*, 322–331. [[CrossRef](#)]
21. Kulasinski, K.; Salmén, L.; Derome, D.; Carmeliet, J. Moisture Adsorption of Glucomannan and Xylan Hemicelluloses. *Cellulose* **2016**, *23*, 1629–1637. [[CrossRef](#)]
22. Einfeldt, J.; Meißner, D.; Kwasniewski, A. Polymerdynamics of Cellulose and Other Polysaccharides in Solid State-Secondary Dielectric Relaxation Processes. *Prog. Polym. Sci.* **2001**, *26*, 1419–1472. [[CrossRef](#)]
23. Davison, B.H.; Pu, Y.; Vural, D.; Parks, J.M.; Sokolov, A.P.; Petridis, L.; Mamontov, E.; Ragauskas, A.J.; Smith, J.C.; Pingali, S.V.; et al. Impact of Hydration and Temperature History on the Structure and Dynamics of Lignin. *Green Chem.* **2018**, *20*, 1602–1611.
24. O'Neill, H.; Pingali, S.V.; Petridis, L.; He, J.; Mamontov, E.; Hong, L.; Urban, V.; Evans, B.; Langan, P.; Smith, J.C.; et al. Dynamics of Water Bound to Crystalline Cellulose. *Sci. Rep.* **2017**, *7*, 1–13. [[CrossRef](#)] [[PubMed](#)]
25. Guo, X.; Qing, Y.; Wu, Y.; Wu, Q. Molecular Association of Adsorbed Water with Lignocellulosic Materials Examined by Micro-FTIR Spectroscopy. *Int. J. Biol. Macromol.* **2016**, *83*, 117–125. [[CrossRef](#)] [[PubMed](#)]
26. Plaza, N.Z. Neutron Scattering Studies of Nano-Scale Wood-Water Interactions. Ph.D. Thesis, University of Wisconsin–Madison, Madison, WI, USA, August 2017.
27. Martínez-Sanz, M.; Gidley, M.J.; Gilbert, E.P. Application of X-Ray and Neutron Small Angle Scattering Techniques to Study the Hierarchical Structure of Plant Cell Walls: A Review. *Carbohydr. Polym.* **2015**, *125*, 120–134. [[CrossRef](#)] [[PubMed](#)]
28. Wiedenhoef, A.C.; Miller, R.B. Structure and Function of Wood. In *Handbook of Wood Chemistry and Wood Composites*; Rowell, R.M., Ed.; CRC Press: Boca Raton, FL, USA, 2005; pp. 9–32.
29. Rowell, R.; Pettersen, R.; Han, J.S.; Rowell, J.S.; Tshabalala, M. Cell Wall Chemistry. In *Handbook of Wood Chemistry and Wood Composites*; CRC Press: Boca Raton, FL, USA, 2005; pp. 35–74.
30. Englund, E.T.; Thygesen, L.G.; Svensson, S.; Hill, C.A.S. A Critical Discussion of the Physics of Wood-Water Interactions. *Wood Sci. Technol.* **2013**, *47*, 141–161. [[CrossRef](#)]
31. Wada, M.; Nishiyama, Y.; Chanzy, H.; FForsyth, T.; Langan, P. The Structure of Celluloses. *Int. Cent. Diffraction* **2008**, *51*, 138–144. [[CrossRef](#)]
32. Nishiyama, Y.; Sugiyama, J.; Chanzy, H.; Langan, P. Crystal Structure and Hydrogen Bonding System in Cellulose I $\alpha$  from Synchrotron X-Ray and Neutron Fiber Diffraction. *J. Am. Chem. Soc.* **2002**, *124*, 9074–9082. [[CrossRef](#)]
33. Sugiyama, J.; Vuong, R.; Chanzy, H. Electron Diffraction Study on the Two Crystalline Phases Occurring in Native Cellulose from an Algal Cell Wall. *Macromolecules* **1991**, *24*, 4168–4175. [[CrossRef](#)]

34. Driemeier, C.; Francisco, L.H. X-Ray Diffraction from Faulted Cellulose I Constructed with Mixed I $\alpha$ –I $\beta$  Stacking. *Cellulose* **2014**, *21*, 3161–3169. [[CrossRef](#)]
35. Nishiyama, Y.; Johnson, G.P.; French, A.D.; Forsyth, V.T.; Langan, P. Neutron Crystallography, Molecular Dynamics, and Quantum Mechanics Studies of the Nature of Hydrogen Bonding in Cellulose I $\beta$ . *Biomacromolecules* **2008**, *9*, 3133–3140. [[CrossRef](#)]
36. Abe, K.; Yamamoto, H. Change in Mechanical Interaction between Cellulose Microfibril and Matrix Substance in Wood Cell Wall Induced by Hygrothermal Treatment. *J. Wood Sci.* **2006**, *52*, 107–110. [[CrossRef](#)]
37. Zhao, Z.; Crespi, V.H.; Kubicki, J.D.; Cosgrove, D.J.; Zhong, L. Molecular Dynamics Simulation Study of Xyloglucan Adsorption on Cellulose Surfaces: Effects of Surface Hydrophobicity and Side-Chain Variation. *Cellulose* **2014**, *21*, 1025–1039. [[CrossRef](#)]
38. Agarwal, U.P.; Reiner, R.R.; Ralph, S.A. Estimation of Cellulose Crystallinity of Lignocelluloses Using Near-IR FT-Raman Spectroscopy and Comparison of the Raman and Segal-WAXS Methods. *J. Agric. Food Chem.* **2013**, *61*, 103–113. [[CrossRef](#)] [[PubMed](#)]
39. Larsson, P.T.; Wickholm, K.; Iversen, T. A CP/MAS <sup>13</sup>C NMR Investigation of Molecular Ordering in Celluloses. *Carbohydr. Res.* **1997**, *302*, 19–25. [[CrossRef](#)]
40. Wiedenhoef, A.C. Structure and Function of Wood. In *Wood handbook: Wood as an Engineering Material*; U.S. Dept. of Agriculture, Forest Service, Forest Products Laboratory: Madison, WI, USA, 2010; pp. 9–33.
41. Scheller, H.V.; Ulvskov, P. Hemicelluloses. *Annu. Rev. Plant Biol.* **2010**, *61*, 263–289. [[CrossRef](#)] [[PubMed](#)]
42. Sun, R.C.; Sun, X.F.; Tomkinson, J. Hemicelluloses and Their Derivatives. *ACS Sym.* **2003**, *846*, 2–22.
43. Terrett, O.M.; Dupree, P. Covalent Interactions between Lignin and Hemicelluloses in Plant Secondary Cell Walls. *Curr. Opin. Biotechnol.* **2019**, *56*, 97–104. [[CrossRef](#)] [[PubMed](#)]
44. Rowell, R.; Pettersen, R.; Tshabalala, M. Cell Wall Chemistry. In *Handbook of Wood Chemistry and Wood Composites*, 2nd ed.; CRC Press: Boca Raton, FL, USA, 2012; pp. 33–72. ISBN 9781439853801.
45. Hansen, C.M.; Björkman, A. The Ultrastructure of Wood from a Solubility Parameter Point of View. *Holzforschung* **1998**, *52*, 335–344. [[CrossRef](#)]
46. Åkerholm, M.; Salmén, L. Interactions between Wood Polymers Studied by Dynamic FT-IR Spectroscopy. *Polymer (Guildf)* **2001**, *42*, 963–969. [[CrossRef](#)]
47. Busse-Wicher, M.; Gomes, T.C.F.; Tryfona, T.; Nikolovski, N.; Stott, K.; Grantham, N.J.; Bolam, D.N.; Skaf, M.S.; Dupree, P. The Pattern of Xylan Acetylation Suggests Xylan May Interact with Cellulose Microfibrils as a Twofold Helical Screw in the Secondary Plant Cell Wall of Arabidopsis Thaliana. *Plant J.* **2014**, *79*, 492–506. [[CrossRef](#)]
48. Rowell, R.M.; Service, F. Moisture Sorption Properties of Acetylated Lignocellulosic Fibers. In *Proceedings of the 10th Cellulose Conference*; Schuerch, C., Ed.; John Wiley & Sons, Inc.: Syracuse, NY, USA, 1989; pp. 343–355.
49. Duval, A.; Lawoko, M. A Review on Lignin-Based Polymeric, Micro- and Nano- Structured Materials. *React. Funct. Polym.* **2014**, *85*, 78–96. [[CrossRef](#)]
50. Terashima, N.; Yoshida, M.; Hafrén, J.; Fukushima, K.; Westermarck, U. Proposed Supramolecular Structure of Lignin in Softwood Tracheid Compound Middle Lamella Regions. *Holzforschung* **2012**, *66*, 907–915. [[CrossRef](#)]
51. Besombes, S.; Mazeau, K. The Cellulose/Lignin Assembly Assessed by Molecular Modeling. Part 2: Seeking for Evidence of Organization of Lignin Molecules at the Interface with Cellulose. *Plant Physiol. Biochem.* **2005**, *43*, 277–286. [[CrossRef](#)] [[PubMed](#)]
52. Cox, J.; McDonald, P.J.; Gardiner, B.A. A Study of Water Exchange in Wood by Means of 2D NMR Relaxation Correlation and Exchange. *Holzforschung* **2010**, *64*, 259–266. [[CrossRef](#)]
53. Zelinka, S.L.; Lambrecht, M.J.; Glass, S.V.; Wiedenhoef, A.C.; Yelle, D.J. Examination of Water Phase Transitions in Loblolly Pine and Cell Wall Components by Differential Scanning Calorimetry. *Thermochimica Acta* **2012**, *533*, 39–45. [[CrossRef](#)]
54. Etzler, F.M. A comparison of the properties of vicinal water in silica, clay, wood, cellulose and other polymeric materials. In *Water Relationships in Foods*; Springer: Boston, MA, USA, 1991; pp. 805–822.
55. Mantanis, G.I.; Young, R.A.; Rowell, R.M. Swelling of Wood Part III. Effect of Temperature and Extractives on Rate and Maximum Swelling. *Holzforschung* **1995**, *49*, 239–248. [[CrossRef](#)]
56. Kirker, G.T.; Blodgett, A.B.; Arango, R.A.; Lebow, P.K.; Clausen, C.A. The Role of Extractives in Naturally Durable Wood Species. *Int. Biodeterior. Biodegrad.* **2013**, *82*, 53–58. [[CrossRef](#)]

57. Almeida, G.; Gagné, S.; Hernández, R.E. A NMR Study of Water Distribution in Hardwoods at Several Equilibrium Moisture Contents. *Wood Sci. Technol.* **2007**, *41*, 293–307. [[CrossRef](#)]
58. Sugino, H.; Sugimoto, H.; Miki, T.; Kanayama, K. Fine structure changes of wood during moisture adsorption and desorption process analyzed by X-ray diffraction measurement. *J. Jpn. Wood Res. Soc.* **2007**, *53*, 82–89. [[CrossRef](#)]
59. Agarwal, U.P.; Ralph, S.A.; Baez, C.; Reiner, R.S.; Verrill, S.P. Effect of Sample Moisture Content on XRD-Estimated Cellulose Crystallinity Index and Crystallite Size. *Cellulose* **2017**, *24*, 1971–1984. [[CrossRef](#)]
60. Kljun, A.; Benians, T.A.S.; Goubet, F.; Meulewaeter, F.; Knox, J.P.; Blackburn, R.S. Comparative Analysis of Crystallinity Changes in Cellulose I Polymers Using ATR-FTIR, X-Ray Diffraction, and Carbohydrate-Binding Module Probes. *Biomacromolecules* **2011**, *12*, 4121–4126. [[CrossRef](#)] [[PubMed](#)]
61. Ahvenainen, P.; Kontro, I.; Svedström, K. Comparison of Sample Crystallinity Determination Methods by X-Ray Diffraction for Challenging Cellulose I Materials. *Cellulose* **2016**, *23*, 1073–1086. [[CrossRef](#)]
62. Heiner, A.P.; Kuutti, L.; Teleman, O. Comparison of the Interface between Water and Four Surfaces of Native Crystalline Cellulose by Molecular Dynamics Simulations. *Carbohydr. Res.* **1998**, *306*, 205–220. [[CrossRef](#)]
63. Einfeldt, J.; Meißner, D.; Kwasniewski, A. Molecular Interpretation of the Main Relaxations Found in Dielectric Spectra of Cellulose—Experimental Arguments. *Cellulose* **2004**, *11*, 137–150. [[CrossRef](#)]
64. Kaminski, K.; Kaminska, E.; Ngai, K.L.; Paluch, M.; Włodarczyk, P.; Kasprzycka, A.; Szeja, W. Identifying the Origins of Two Secondary Relaxations in Polysaccharides. *J. Phys. Chem. B* **2009**, *113*, 10088–10096. [[CrossRef](#)] [[PubMed](#)]
65. Thybring, E.E.; Kymäläinen, M.; Rautkari, L. Experimental Techniques for Characterising Water in Wood Covering the Range from Dry to Fully Water-Saturated. *Wood Sci. Technol.* **2018**, *52*, 297–329. [[CrossRef](#)]
66. Chen, S.H. Quasi-Elastic and Inelastic Neutron Scattering and Molecular Dynamics of Water at Supercooled Temperature. In *Hydrogen-Bonded Liquids*; Dore, J.C., Teixeira, J., Eds.; Kluwer Academic Publishers: Dordrecht, The Netherlands, 1989; pp. 289–332.
67. Gao, X.; Zhuang, S.; Jin, J.; Cao, P. Bound Water Content and Pore Size Distribution in Swollen Cell Walls Determined by NMR Technology. *Bioresources* **2015**, *10*, 8208–8224. [[CrossRef](#)]



© 2019 by the author. Licensee MDPI, Basel, Switzerland. This article is an open access article distributed under the terms and conditions of the Creative Commons Attribution (CC BY) license (<http://creativecommons.org/licenses/by/4.0/>).